Dynamics of ions produced by laser ablation of several metals at 193 nm

G. Baraldi, A. Perea, and C. N. Afonso

Related Articles

Influence of excited state spatial distributions on plasma diagnostics: Atmospheric pressure laser-induced He-H2 plasma
J. Appl. Phys. 112, 083302 (2012)

Characterizing the energy distribution of laser-generated relativistic electrons in cone-wire targets
Phys. Plasmas 19, 103108 (2012)

Verification of the physical mechanism of THz generation by dual-color ultrashort laser pulses
Appl. Phys. Lett. 101, 161104 (2012)

ORION laser target diagnostics
Rev. Sci. Instrum. 83, 10D732 (2012)

Target normal sheath acceleration sheath fields for arbitrary electron energy distribution
Phys. Plasmas 19, 083115 (2012)
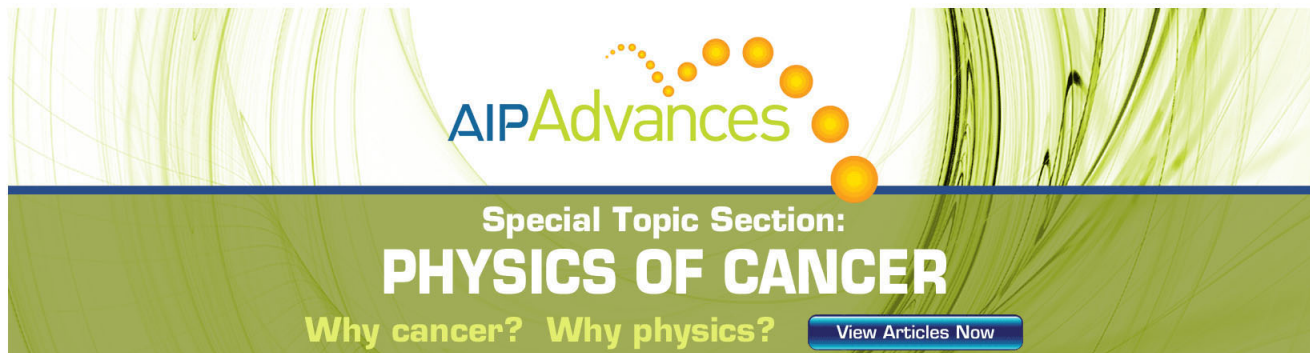
Additional information on J. Appl. Phys.

Dynamics of ions produced by laser ablation of several metals at 193 nm

G. Baraldi,[a)] A. Perea, and C. N. Afonso

Laser Processing Group, Instituto de Óptica, CSIC, Serrano 121, 28006 Madrid, Spain

This work reports the study of ion dynamics produced by ablation of Al, Cu, Ag, Au, and Bi targets using nanosecond laser pulses at 193 nm as a function of the laser fluence from threshold up to 15 J cm^{-2}. An electrical (Langmuir) probe has been used for determining the ion yield as well as kinetic energy distributions. The results clearly evidence that ablation of Al shows unique features when compared to other metals. The ion yield both at threshold (except for Al, which shows a two-threshold-like behavior) and for a fixed fluence above threshold scale approximately with melting temperature of the metal. Comparison of the magnitude of the yield reported in literature using other wavelengths allows us to conclude its dependence with wavelength is not significant. The evolution of the ion yield with fluence becomes slower for fluences above 4–5 J cm^{-2} with no indication of saturation suggesting that ionization processes in the plasma are still active up to 15 J cm^{-2} and production of multiple-charged ions are promoted. This dependence is mirrored in the proportion of ions with kinetic energies higher than 200 eV. This proportion is not significant around threshold fluence for all metals except for Al, which is already 20%. The unique features of Al are discussed in terms of the energy of laser photons (6.4 eV) that is enough to induce direct photoionization from the ground state only in the case of this metal. © *2011 American Institute of Physics*. [doi:10.1063/1.3549159]

INTRODUCTION

Pulsed laser deposition has proved to be an attractive technique for producing thin films of many materials, including metal systems. It is generally accepted that the special features or improved performance relate to their different microstructure when compared to systems produced using conventional techniques.[1–4] The high kinetic energy of species arriving to the substrate is the most widely reported reason for these differences, but their presence can also lead to undesired processes such as resputtering of deposited species,[4–7] mixing or alloying at the interface,[8] or subsurface implantation.[4,6,7] The complete origin of many of these processes is not yet well understood in part due to the lack of detailed information on the actual kinetic energy of the species reaching the substrate in a broad laser fluence range, since average or mean values are typically reported rather than velocity distributions.

Ions are the species in the laser induced plasma having the higher kinetic energies,[9–11] and considered responsible for sputtering or implantation at substrate level during pulsed laser deposition.[4,6,7] The ionization fraction is determined by the fluence and wavelength of the laser used for ablation.[12] Ions become a fraction as high as 50% of the total amount of species for relatively low fluence (2–3 J cm^{-2}) for the case of Ag (Ref. 13) or Au (Ref. 11) and this fraction increases as fluence increases. With some exceptions,[5,9,10,14] most of the studies only report mean kinetic energies of ions. Instead, processes at substrate level have been related to ions having kinetic energies higher than 200 eV.[11] In addition, mean kinetic energies generally vary little with fluence,[10] while distributions are known to expand significantly toward high kinetic energy values up to 1 keV as fluence is increased.[9–11,14]

There are several publications reporting studies related to plasmas produced by laser ablation. Most of them use lasers with wavelengths in the near UV (355 nm), visible (532 nm) or infrared, i.e., photon energies that are generally well below the ionization potential of most metals and even below the binding energy of many metals (>3 eV/atom). The total ablated yield for several metals has been reported to decrease linearly as melting temperature[13] or cohesive energy[15] increases when ablating with 2.0 J cm^{-2} at 355 nm. The ion yield has been reported for a reduced number of metals and it was similarly reported that the yield is substantially higher for the most volatile (Bi) metal.[13] Studies of ions produced by ablation of Al with 532 and 355 nm with fluences up to 66 J cm^{-2} report the existence of saturation effects in the total yield at high fluences.[14,16] A comparison study of the ablation threshold of several materials including metals at three wavelengths, namely 1064, 532, and 248 nm, leads one to conclude that the prevalent mechanism for ablation differs from thermal when photon energy becomes higher than the binding energy of the target material.[17] In addition, photoionization of Cu neutrals was reported to occur at lower fluences for 193 nm than for 351 nm, supporting the existence of single photon ionization even at a photon energy smaller than the ionization potential.[12] In spite of the reduced number of reports comparing different laser wavelengths, it seems clear that the plasma features produced at 193 nm cannot directly be extrapolated from those produced at longer wavelengths.

The aim of this work is to determine the yield and kinetic energy distribution of ions produced by laser ablation

---

a)Author to whom correspondence should be addressed. Electronic mail: giorgiob@io.cfmac.csic.es.

© 2011 American Institute of Physics

at 193 nm of metal targets in a wide fluence interval. We have selected to study Au, Ag, Cu, and Bi because on the one hand, several reports on the production of nanoparticles of these metals by pulsed laser deposition have emphasized the importance of high energetic ions ($\geq$200 eV) in determining their structural features.[4,7,11,18,19] On the other hand, reports on kinetic energy distributions upon ablation at 193 nm are limited to Au (Ref. 11) and Cu.[10] In addition, we have chosen to study Al because it has been the most widely studied metal using not only 193 nm (Ref. 10) but mainly other wavelengths in the visible and near infrared[13,14,16,17,20] and thus makes a very good case for comparing to results reported in literature.

EXPERIMENTAL PROCEDURES

Laser ablation of targets was performed using an ArF laser ($\lambda = 193$ nm, $\tau = 20$–25 ns full width at half maximum). Laser beam is focused on the target surface at an angle of incidence of 45° with respect to the target normal. Targets are located in a vacuum chamber kept at a pressure of $\approx 10^{-5}$ mbar. Laser fluence is varied from plasma formation threshold up to 15 J cm^{-2}. Values are obtained by dividing the energy at the target site by the spot area determined by measuring the ablated area in an aluminum foil located at the target site.

A Langmuir probe (LP), placed opposite to the target at a distance of 40 mm, is used to collect the ions generated by laser ablation. LP consists of a small squared Cu electrode of 1.07 mm^2 area and with its rear side electrically insulated. The LP signal is injected into a Koopmann circuit[21] that is characterized by a high pass filter ($R = 5.7\Omega$, $C = 10$ μF) to stabilize the incoming LP signal and a bias voltage of -10 V to ensure that only ions are collected. The current transient is recorded by a digital oscilloscope that is triggered by a fast photodiode. Series of transients obtained at 1 Hz are recorded in each point of the target. Similar to earlier reports for the case of Au (Ref. 11) and other metals,[22] first transients show, in addition to the characteristic peak related to metal ions, a narrow peak at short times that disappears after few laser shots. This spurious peak is related to contamination of target surface and all results reported in this work correspond to transients recorded from clean targets.

Assuming that ions are single-ionized, ion current density transients $J(t)$ are obtained from current transients $I(t)$ as:

$$J(t) = I(t)/(S \cdot e), \qquad (1)$$

where S is the LP area and e is the charge of electron. The number of ions collected by the LP per unit area and per pulse (ion yield) is obtained by time integrating $J(t)$ and kinetic energy distribution of ions [$N(E)$] are calculated using[11]:

$$N(E) = J(t) \cdot |Jac(E)|, \qquad (2)$$

where $|Jac(E)| = t^3/(md^2)$ is the Jacobian needed to convert a time t dependent distribution to a kinetic energy $E = 0.5\,m(d/t)^2$ dependent distribution, where m is the atomic weight of the
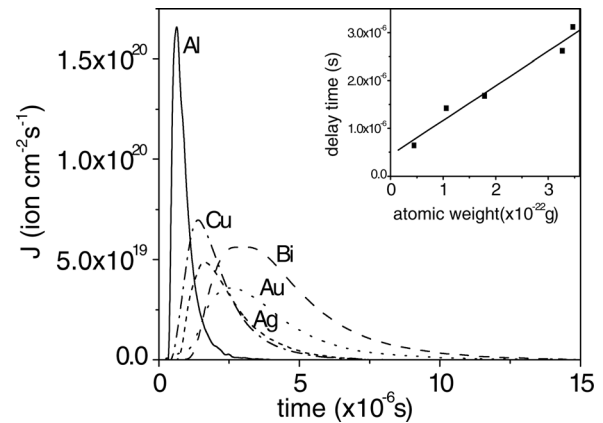

FIG. 1. Current density transients obtained by ablating all metal targets with a laser fluence of 8 J cm^{-2}. The inset shows the time delay at which the maximum occurs with respect to the laser pulse as a function of the metal atomic weight. Solid line is a linear fit of experimental data.

ion considered and d is the target to probe distance.[11] We have verified the $1/d^2$ dependence of the signal collected by the LP and all results reported in this work refer to $d = 40$ mm.

RESULTS

Figure 1 shows current density transients obtained by ablation of all metals studied in this work at a laser fluence of 8 J cm^{-2}. While transient shape is very similar for all metals, a fast rise followed by a slower decay that reaches zero, the maximum of each curve corresponds to a different time delay. The inset shows the instant at which maximum is reached as a function of the atomic weight of the metal (Table I) where it is seen it follows a linear dependence.

Figure 2 shows the ion yield as a function of laser fluence. All metals show a similar behavior, i.e., the amount of ions increases when laser fluence increases. A change of slope is observed in all cases for fluences around 4–5 J cm^{-2}, the slope becoming smoother for higher fluences. All metals show similar yield values with the exception of Bi, which shows almost double values.

In spite of these similarities, there are significant differences for fluences near threshold as seen in Fig. 3, which shows a magnification of Fig. 2 in the low fluence region. Whereas the yield of Bi, Ag, Au, and Cu shows an almost linear behavior whose cutoff with the horizontal axis provides the threshold fluence for ion ejection, Al exhibits a distinct behavior that is highlighted by a dashed line. For fluences down to 1.4 J cm^{-2}, it follows a linear behavior

TABLE I. Metals studied in this work and their atomic weight (AW), melting temperature (T_m), ionization potential from ground state (IP), and energy of first and second excited states (ESE) (Ref. 25); the two values given in some cases account for multiple states.

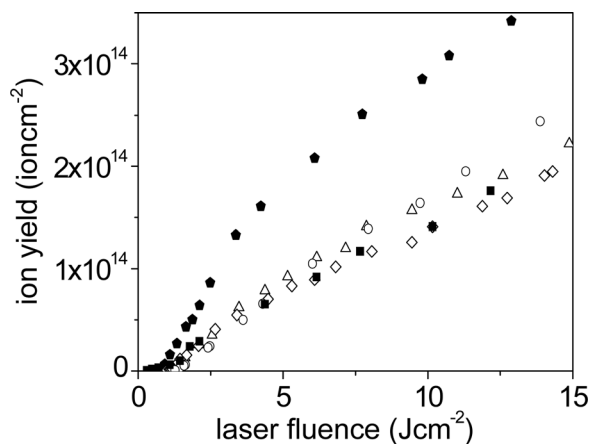| Metal	AW ($\times 10^{-22}$ g)	T_m (K)	1st IP (eV)	1st ESE (eV)	2nd ESE (eV)
Al	0.448	933	5.98	3.14	3.6
Cu	1.055	1357	7.72	1.4–1.6	3.8
Ag	1.791	1234	7.57	3.7	3.7–4.3
Au	3.271	1337	9.22	1.1–2.6	4.6–5.1
Bi	3.470	544	7.28	1.4–1.9	2.7–4.1

FIG. 2. Ion yield as a function of laser fluence recorded upon ablation of Al (■), Cu (○), Ag (◇), Au (Δ) and Bi (closed pentagon).

with a slope similar to that of other metals. Its extrapolation to the horizontal axis provides what we will refer to from now on as the *apparent* threshold. For smaller fluences, the yield follows a linear dependence with a much lower slope, leading to what we will refer to from now on as the *real* threshold. A log–log plot of threshold values as a function of melting temperature of metal is shown in Fig. 4(a). It is seen that all metals, together with the apparent threshold for Al, follow an increasing linear dependence with melting temperature, while the real threshold for Al provides a much smaller value that is even smaller than that of the smallest melting point metal (Bi). The log–log dependence of the ion yield on melting temperature is shown in Fig. 4(b) for two selected fluences, namely 2 and 10 J cm^{-2}. In those cases for which there was no experimental point at the chosen fluence, the values have been extrapolated assuming a linear dependence between the two neighboring experimental values. The results show that ion yield decreases as melting temperature increases and the dependence becomes slightly smoother as fluence increases.
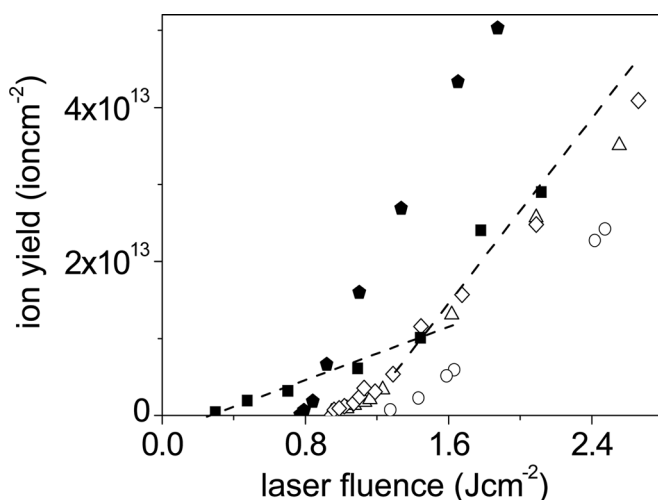

FIG. 3. Magnification of ion yield in Fig. 2 for low fluences, upon ablation of Al (■), Cu (○), Ag (◇), Au (Δ) and Bi (closed pentagon). The dashed line is a guideline for the behavior of the ion yield in the case of Al that illustrates the way the apparent and real threshold values (see the text) are determined.
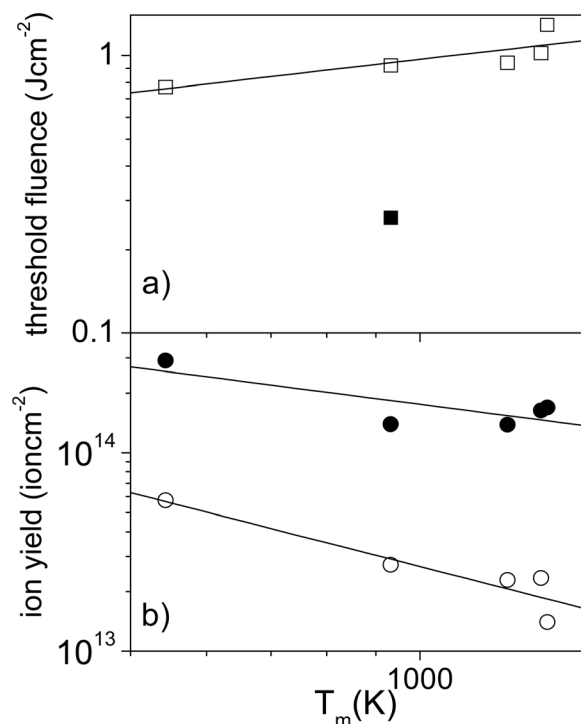

FIG. 4. Log–log plot as a function of melting temperature of the metal of: (a) Fluence threshold for ions where both apparent (■) and real (□) thresholds for Al are included. (b) Ion yield at 2 J cm^{-2} (○) and 10 J cm^{-2} (●). The lines are guidelines.

Figure 5 shows the kinetic energy distributions calculated from current transients for Au at three different laser fluences, namely 2.5, 9, and 15 J cm^{-2}. As shown in an earlier work,[11] $N(E)$ is always characterized by a maximum at relatively low energy ($\approx$50 eV) followed by a long decay. The position of the maximum shows no significant changes with laser fluence. Instead, the maximum intensity decreases and the decays extend into the high kinetic energy region as fluence is increased.

Figure 6 allows comparing the kinetic energy distributions of different metals obtained for a fixed laser fluence of 2.5 J cm^{-2}. The features are very similar to those described for Au in Fig. 5, i.e., a maximum at relatively low energy followed by a long decay. Furthermore, the maximum is
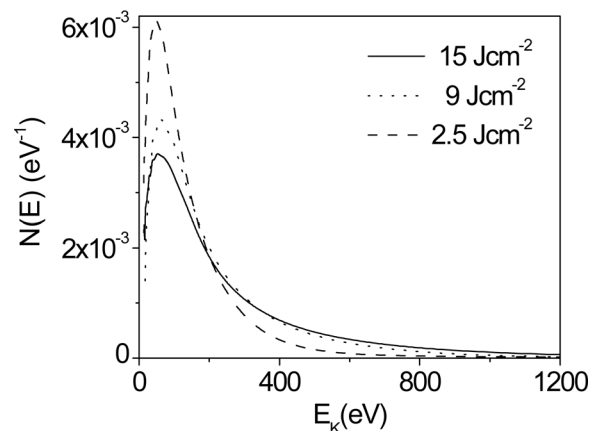

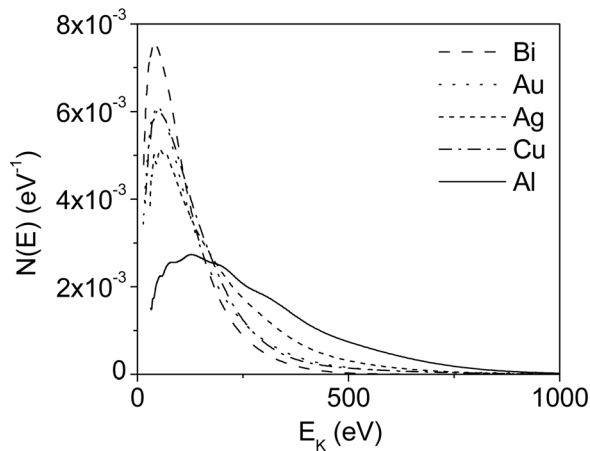FIG. 5. Ion kinetic energy distribution obtained by ablating Au target at three different laser fluences: 2.5, 9, and 15 J cm^{-2}.

FIG. 6. Ion kinetic energy distribution obtained by ablating all metal targets with a fluence of 2.5 J cm^{-2}.

around a similar low energy value (≈ 50 eV) for all metals studied except for Al, which shows its maximum at around ≈ 130 eV together with a stronger contribution of energetic ions as evidenced by the fact that the long decay extends up to ≈ 1000 eV. Figure 7 quantifies the latter feature by showing the percentage of ions with kinetic energy $E_k > 200$ eV as a function of fluence; these ions will be referred to from now on as *energetic* ions. It is seen that they are at least twice for Al than for other metals irrespective of laser fluence. Further, for fluences for which most metals show no significant number of them, Al already shows that 20% of ions are energetic ions. Figure 7 also shows that the amount of energetic ions increases as fluence increases as expected and mirrors the evolution of the ion yield dependence on fluence shown in Fig. 2. There is also a change of slope around 4–5 J cm^{-2}, the slope becoming smoother for the higher fluences. In addition, it is worth noting that whereas Bi is the metal showing the highest ion yield in Fig. 2, it is the one showing the lowest proportion of energetic ions.

DISCUSSION

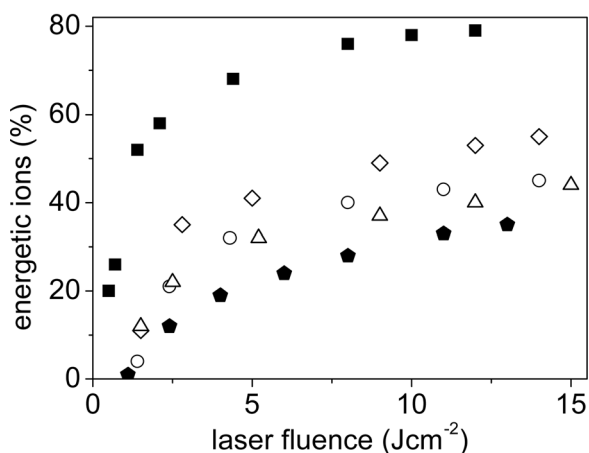Time of flight distributions of ions after ablation of Al, Bi, and Ag at 355 nm and Al and Cu at 193 nm have been

FIG. 7. Percentage of ions with kinetic energy higher than 200 eV as a function of laser fluence upon ablation of Al (■), Cu (○), Ag (◇), Au (△), and Bi (closed pentagon).

reported in Refs. 13 and 10, respectively. In all cases, the instant at which maximum is reached increases as the atomic weight increases, as seen in our results shown in the inset of Fig. 1. However, the intensity of Al signals in Ref. 13 is significantly lower than that of Bi, i.e., it follows the opposite behavior to the one shown in Fig. 1, while the relative intensities of Ag and Bi follow a similar trend. Instead, the relative intensities achieved for Al and Cu at 193 nm in Ref. 10 follow the same trend as in Fig. 1. This very simple comparison evidences that the behavior of Al becomes different than that of other metals when using 193 nm photons. The fact that the species produced by ablation of metals and semiconductors in vacuum depends on the laser wavelength has already been pointed out, long wavelengths inducing a sort of evaporation-like process dominated by atomic ejection and short wavelengths inducing photoionization and photochemical processes.[17]

Table I shows the ionization potential from ground (IP) and first and second excited states of all metals studied in this work. It shows that the use of 193 nm (6.4 eV) can only promote direct photoionization in the case of Al and can produce photoionization from first and second excited states in the case of all metals studied. Experiments on ablation of Al and Cu at 351 nm (3.5 eV) provide evidence for photoionization from the first excited state in the case of Al and not in the case of Cu, consistent with the data in Table I.[20] In addition, early work performed in Cu at two different wavelengths, namely 193 nm (6.4 eV) and 351 nm (3.5 eV) have reported photonionization through one and three photon processes, in spite of the ionization potential being approximately 1.3 eV higher than the former photons.[12] More recent results using 193 nm to ablate Al and Cu confirm these findings and provide further support for the high degree of ionization through a variety of processes occurring when using 6.4 eV photons.[10]

The consequences of the laser photon energy being comparable to the ionization potential should be more noticeable near threshold, as evidenced in Fig. 4(a). Results clearly show that Al behaves differently than other metals. The apparent threshold for Al fits well to the threshold for the other studied metals and, similar to the ion yield discussed earlier, it is a metal dependent parameter. It scales with the melting temperature; the lower the melting temperature the lower the threshold. However, the real threshold for Al is much lower than that of other metals. It can thus be concluded that the lower threshold for ions in the case of Al (a factor of 0.3) is due to the existence of photoionization processes caused directly by the laser photons that promote their appearance in the gas phase at much lower fluences than in other metals.

The comparison of kinetic energy distributions of the different studied metals (Fig. 6) also evidences that Al has a distinct behavior: its maximum is shifted toward higher energies and the contribution of energetic ions becomes remarkably higher. Further, the amount of the latter is very high even for fluences at which it is below 10% in the case of the other metals studied. As reported in several works,[9,10,12,23] a charge imbalance occurs in the plasma due to energetic electrons that escape toward the leading edge of the plume.

It produces a high electrical field inside the plasma and makes the distribution of ions forwardly peaked along the direction perpendicular to the target.[9] This field accelerates ions with an acceleration that scales with the ion charge. This effect would thus be more important for Al than for the other studied metals, since triple ionized species have been detected for the former[16] while single or double ionized species have been reported for the latter.[10–12,24] We can thus conclude that the use of laser photons with enough energy for producing direct ionization enhances the degree of ionization of the plasma that consequently shifts the kinetic energy distribution to higher energies due to Coulomb acceleration. Even if in our experimental conditions we are not able to distinguish between single and multiple ionized species, this conclusion together with the fact that the energetic ions (Fig. 7) follow the same trend with fluence as the total yield of ions in Fig. 2, suggest that the still increasing yield after the change of slope is most likely related to the production of multiple-charged ions above 4–5 J cm^{-2}.

The total ablation yield (i.e., the number of ablated atoms per pulse as determined by weight loss and thus accounting for both neutrals and ions) has been reported for several metals as a function of their melting point[13] or cohesive energy.[15] It is shown that the total ablation yield decreases as both parameters increase. Further, the yield decreases approximately one order of magnitude from the most volatile metal (Bi) to the less volatile one studied in this work (Cu). Our results for ion yield shown in Fig. 4(b) for a similar fluence (2 J cm^{-2}) as in Ref. 13 shows a dependence very similar to that shown for the total yield, including a variation close to one order of magnitude. The angular distributions for Al, Ag, and Bi ions were also provided in Ref. 13 for a fluence of 2 J cm^{-2}. The reported ion densities along the direction perpendicular to the target surface are approximately 5×10^{13} ions cm^{-2} for Bi and 1×10^{13} ions cm^{-2} for Al and Ag. If we take into account that their probe–target separation d was 80 mm, ours is 40 mm, and that the probe signal has a $1/d^2$ dependence, we find an excellent agreement between our results and those reported in Ref. 13 despite the different wavelengths used for ablation (193 nm in our work and 355 nm in earlier work). There are two interesting conclusions that could be drawn from this comparison and Fig. 4(b). The first one is that the laser ablation wavelength does not appear to be important in determining the magnitude of the yield for fluences above the threshold. The second conclusion is that the magnitude of the yield is mainly determined by the melting temperature of the metal; the higher the melting temperature the lower the yield. This dependence appears to become smoother as fluence is increased, suggesting that plasma over target processes become of increased importance in the ablation process as fluence is increased.

The amount of ablated material and the efficiency of collisional ionization processes are acknowledged to increase with fluence. It has been reported for the case of Al that ion yield increases with fluence and saturates for fluences higher than ≈ 5 and 6 J cm^{-2} when ablating with 355 and 532 nm laser wavelength, respectively.[16] This saturation was related to the plasma becoming opaque and absorbing the laser light and, interestingly, it is in this regime when multiple ionized

Al^{++} or even Al^{+++} species are observed, mainly upon ablation with 355 nm. The threshold for multiple-charged ions was similarly reported to increase by increasing the charge state for the case of Ta target.[9] Our results in Fig. 2 show that ion yield increases similarly with fluence for low fluence values and a change in slope occurs for fluences close to 4–5 J cm^{-2}. The ion yield remains increasing with fluence, although at a lower rate, after the change of slope, thus evidencing that ionization processes are still active at these high fluences. There are at least three processes that might be contributing to this increase in our case: the high energy of our laser photons that promotes photoionization processes from first and second excited states; the production of multiple-charged ions above 4–5 J cm^{-2} as reported for Al (Ref. 16) and Ta (Ref. 9) that would lead to an "apparent" increase of the yield in our experimental conditions; and dissociation of dimers as reported for the case of Cu$_2$ for fluences higher than 4 J cm^{-2}.

CONCLUSIONS

The main conclusion of this work is that the high photon energy when using a laser at 193 nm for ablation leads to special features in the ion properties of the plasma produced by ablation of metals. This is especially the case for Al, for which its ionization potential is smaller than the laser photon energy and thus direct photoionization processes are possible. This leads to a much lower threshold fluence for ion production in Al than in other metals, as well as a much higher mean kinetic energy and proportion of energetic ions (>200 eV). While most metals show no significant proportion of the latter around threshold fluence, that of Al is already 20%. The high photon energy is also found responsible for the plasma processes still being active for fluences up to 15 J cm^{-2} not only by photoionization of the first and second excited states but also (and most likely by) the production of multiple-charged ions. The amount of ions for fluences above threshold is instead dominated by the target, since it follows a log–log linear dependence with the melting temperature of the metal. This dependence becomes smoother as fluence is increased, confirming that plasma processes are still active and become dominant.

ACKNOWLEDGMENTS

[1]S. Kahl and H-U Krebs, Phys. Rev. B **63**, 172103 (2001).

[2]A. Zenkevich, J. Chevallier, and I. Khabelashvili, Thin Solid Films **311**, 119 (1997).

[3]E. Irissou, B. Le Drogoff, M. Chaker, and D. Guay, Appl. Phys. Lett. **80**, 1716 (2002).

[4]J. Gonzalo, A. Perea, D. Babonneau, C. N. Afonso, N. Beer, J. P. Barnes, A. K. Petford-Long, D. E. Hole, and P. D. Townsend, Phys. Rev. B **71**, 125420 (2005).

[5]R. Jordan, D. Cole, J. G. Lunney, K. Mackay, and D. Givord, Appl. Surf. Phys. **86**, 24 (1995).

[6]K. Sturm and H.-U. Krebs, J. Appl. Phys. **90**, 1061 (2001), and references therein.

[7]A. Suarez-Garcia, J-P. Barnes, R. Serna, A. K. Petford-Long, C. N. Afonso and D. Hole, Mater. Res. Soc. Symp. Proc. (Mater. Res. Soc., Warrendale, PA, 2003), Vol. 780, pp. 3–8.

[8]R. Gupta, M. Weisheit, H.-U. Krebs, and P. Schaaf, Phys. Rev. B **67**, 075402 (2003).

[9]L. Torrisi, F. Caridi, A. Picciotto, D. Margarone, and A. Borrielli, J. Appl. Phys. **100**, 093306 (2006).

[10]F. Claeyssens, S. J. Henley, and M. N. R. Ashfold, J. Appl. Phys. **94**, 4 (2003); an error has been identified in Fig. 2 related to the mean kinetic energy of Al ions as a function of fluence that corresponds to the triangles instead of the circles.

[11]A. Perea, J. Gonzalo, C. Budtz-Jørgensen, G. Epurescu, J. Siegel, C. N. Afonso, and J. García-Lopez, J. Appl. Phys. **104**, 084912 (2008).

[12]R. W. Dreyfus, J. Appl. Phys. **69**, 3 (1991).

[13]B. Thestrup, B. Toftmann, J. Schou, B. Doggett, and J. G. Lunney, Appl. Surf. Phys. **197–198**, 175 (2002).

[14]S. Amoruso, M. Armenante, V. Berardi, R. Bruzzese, R. Velotta, and X. Wang, Appl. Surf. Sci. **127–129**, 1017 (1998).

[15]J. Schou, Appl. Surf. Sci. **255**, 5191 (2009).

[16]S. Amoruso, V. Berardi, R. Bruzzese, R. Capobianco, R. Velotta, and M. Armenante, Appl. Phys. A **62**, 533 (1996).

[17]L. Torrisi, A. Borrielli, and D. Margarone, Nucl. Instrum. Methods Phys. Res. B **255**, 373 (2007).

[18]J. P. Barnes, A. K. Petford-Long, R. C. Doole, R. Serna, J. Gonzalo, A. Suarez-Garcia, C. N. Afonso, and D. Hole, Nanotechnology **13**, 465 (2002).

[19]R. Serna, A. Suarez-Garcia, C. N. Afonso, and D. Babonneau, Nanotechnology **17**, 4588 (2006).

[20]S. Amoruso, V. Berardi, R. Bruzzese, R. Velotta, N. Spinelli, and X. Wang, Appl. Surf. Sci. **138–139**, 250 (1999).

[21]D. W. Koopman, Phys. Fluids **14**, 1707 (1971).

[22]G. O. Williams, G. M. O'Connor, P. T. Mannion, and T. J. Glynn, Appl. Surf. Sci. **254**, 5921 (2008).

[23]N. M. Bulgakova, A. V. Bulgakov, and O. F. Bobrenok, Phys. Rev. E **62**, 5624 (2000).

[24]M. E. Sherrill, R. C. Mancini, J. E. Baily, A. Filuk, B. Clark, P. Lake, and J. Abdallah, Jr., Rev. Sci. Instrum. **72**, 1 (2001).

[25]Data taken from http://environmentalchemistry.com/yogi/periodic/1stionization.html and http://physics.nist.gov/PhysRefData/ASD/levels_form.html.